S-Band Radar Altimeter

By

Bobby Sommers (sommers7)
Elliot Rubin (earubin2)
Rayan Nehme (rayannn2)

Final Report for ECE 445, Senior Design, Spring 2024
TA: Koushik Udayachandran
Professor: Viktor Gruev

01 May 2024
Project 18

Abstract

This document describes the design, fabrication, and subsequent testing of our radar altimeter project. The radar altimeter provides an alternative to traditional GPS or optical sensing techniques commonly used by consumer drones. This report will enumerate the design process of the radar altimeter, including the derivation of system and subsystem requirements, simulation, and verification of each component. Finally, we discuss outcomes, cost, and eventual next steps towards a production-ready version of the radar altimeter.

Contents

1. Introduction

1.1 Problem

Consumer drones often rely on GPS or IR sensing for navigation and terrain avoidance. GPS, while reliable outdoors, requires line of sight to the sky and will not function properly in highly urban environments or indoor spaces. IR sensing reliably works indoors or in confined spaces, but its performance quickly degrades with increased distance, surface reflectivity, and drastic light changes [8], among other conditions commonly faced by pilots. Alternative sensor technologies such as lidar or mmWave radar improve on these issues to some degree, but are prohibitively expensive for consumers and suffer from low maximum range.

1.2 Solution

Our solution implements a radar altimeter operating in the S-band (2.25 GHz - 2.5 GHz), which can be mounted on large consumer drones. The radar uses an internal microcontroller and frequency modulator to generate FMCW (frequency-modulated continuous-wave) signals of variable bandwidth for different distances. On the receiver side, the radar uses a LNA (low-noise amplifier), a mixer, and op-amps for the IF (intermediate frequency) filter. For transmission and reception, the radar relies on two small antennas. Inside the radar, a mixer multiplies the transmitted and received signals to produce a difference signal, giving us information about the distance to the target (terrain). The distance is calculated using standard formulae for FMCW radars and is stored to an onboard SD card. To assess the precision and accuracy of the radar, an onboard barometric sensor will also be used and its data will be written to the SD card as well for post processing.

1.3 Visual Aid

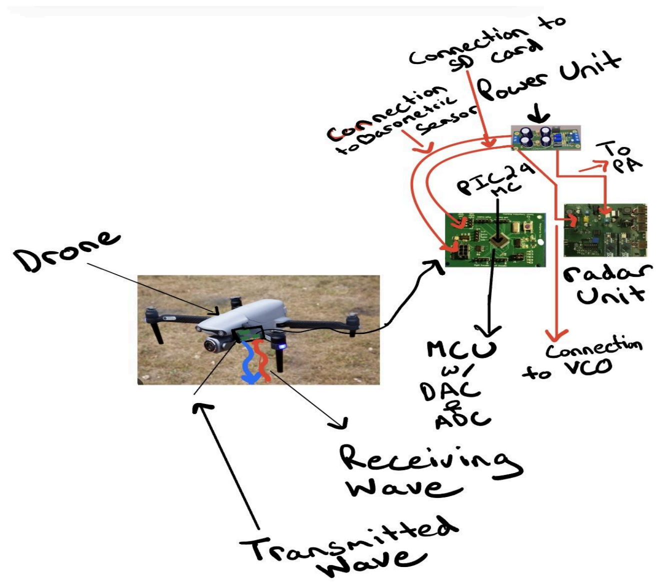

Figure 1: Visual Aid

1.4 Requirements

We derived the following high-level requirements to ensure the success of our radar altimeter:

1. The radar must have a maximum detection range greater than 20 m.
2. The receiver noise figure must not exceed 10 dB.
3. The radar must have a range resolution of 1.5 m or better.

2. Design

2.1 Design Overview

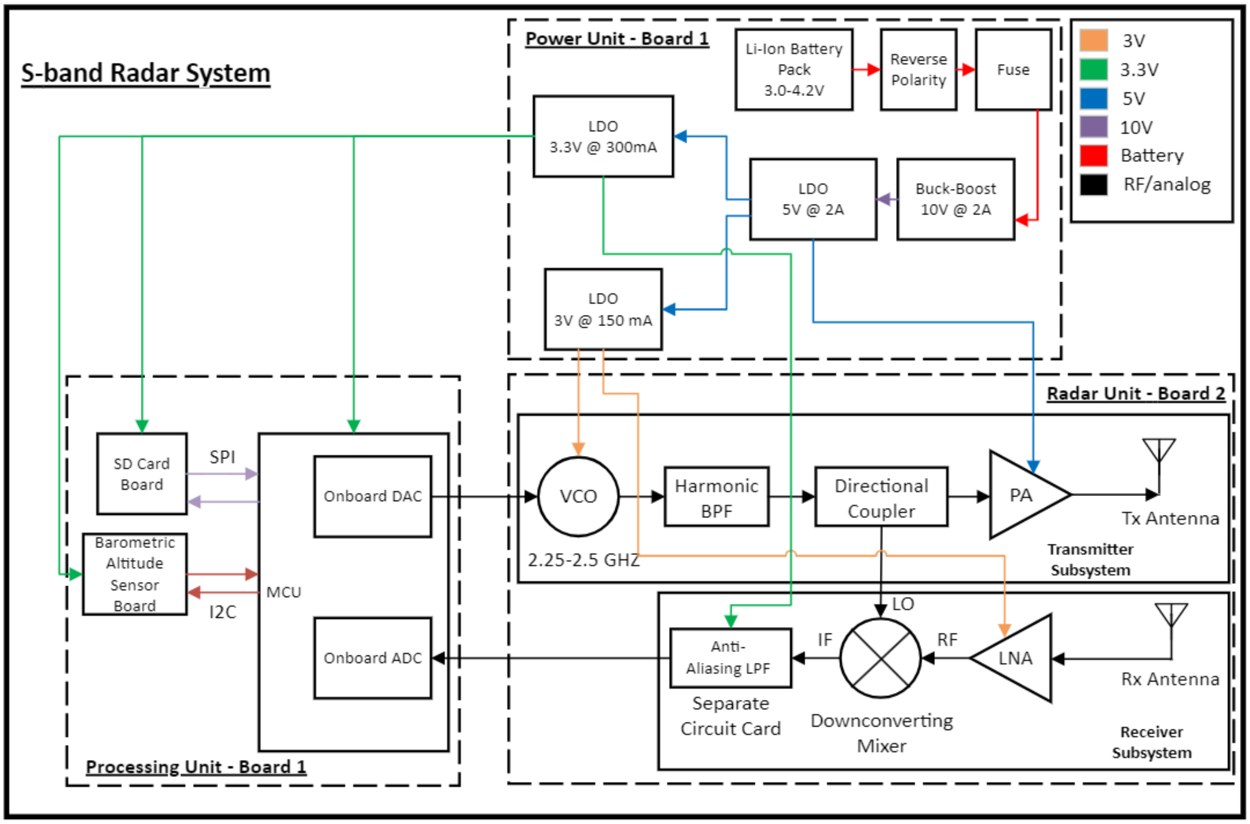

Figure 2: Full System Block Diagram

Our design consists of 3 subsystems: processing unit, power unit, and radar unit. The processing unit is responsible for creating a triangle waveform that is fed into the VCO (voltage controlled oscillator) input. This allows for an FMCW wave to be created which is integral to the function of the radar unit. The processing unit also records data coming through the Rx (receiver) chain of the radar unit to be recorded for post processing to compare against the barometric readings. The power unit is responsible for providing power to all active components of the design. This includes the various voltage inputs to the MCU, SD card board, barometric sensor, VCO, PA (power amplifier), and LNA. This is accomplished through the use of 3 LDOs and a switching converter. A lithium-ion battery was originally part of the design but was ultimately not included in the final product. The radar unit Tx (transmitter) chain is responsible for filtering and power amplifying the FMCW signal from the VCO that will lead into an antenna. The Rx chain is responsible for amplifying the received signal and mixing it with the transmit signal. This mixing function will output a sum and difference signal that the LPF will only keep the difference. This process will allow us to determine the distance to the ground through the equation [3]:

$$R = \frac{Tcf_r}{2(f_{max} - f_{min})} \quad (1)$$

where T is the time for the triangle waveform to reach a maximum value, c is the speed of light, f_r is the beat frequency, f_{max} is the maximum frequency of the FMCW signal, and f_{min} is the minimum frequency of the FMCW signal. The beat frequency can be determined through the relation [3]:

$$f_r = \frac{\left|f_{bu} + f_{bd}\right|}{2} \quad (2)$$

where f_{bu} is the difference of the transmit at receive signal during the rising edge of the FMCW signal, and f_{bd} is the difference of the transmit at receive signal during the falling edge of the FMCW signal.

2.1.1 Changes to Design

The original design described in section 2.1 required significant changes to both the radar unit and the processing unit in order to function properly. Originally, the radar unit consisted of an RF PCB and an IF circuit card for filtering the baseband beat frequency. However, oscillation in both the transmitter's PA and the receiver's LNA necessitated a redesign. This oscillation was likely caused by improperly placed lumped components and untuned trace lengths at both the inputs and outputs of the amplifiers. As a result, unstable source and load impedances were presented to the amplifiers, causing them to oscillate and fail. Since the only functional part of the first two revisions of our RF PCBs was the VCO, we decided to design a standalone board that could be populated with either the amplifier, the mixer, or a power divider. Ultimately, we only populated the amplifier section of this board for use in the transmitter, and instead used an off-the-shelf mixer, LNA, and power divider to create a working system. Additionally, the IF filter required the input signal to be applied with a DC offset, which we discovered after attempting to characterize its frequency response. This, combined with low dynamic range, made the filter unusable in the design, so we did not use it in our demonstration. We also observed a loading effect at the VCO tuning input, which we initially attributed to the op-amp circuitry we placed at the tuning pin. However, we discovered that the microcontroller's DAC output was resistive, creating a voltage divider with the resistor at the op-amp's input. This was mitigated by buffering the DAC output, allowing us to achieve the full VCO sweep bandwidth.

The changes to the power-processing unit (PPU) were primarily driven by our inability to properly configure the PIC microcontroller we chose to use. To this end, we used a Microchip Nano evaluation board instead of our onboard microcontroller. While we observed SPI transmission on a logic analyzer, we were unable to communicate with our SD card module to log data. We also discovered that the onboard ADC could not sample at a high enough frequency to avoid aliasing while also maintaining an adequate data rate for SPI transactions. This issue was observed for SPI running in polling mode and in interrupt mode. We attempted to mitigate this issue by using an Arduino, but were still unable to record ADC data and write it to the SD card via SPI. Finally, we chose not to use a Lithium battery to power our project as we had no way to safely charge it.

2.2 Design Procedure

Radar architectures can be distinguished by what type of waveform they employ. There is CW (continuous wave) radar, which uses a pure tone for measurement. The drawback of a CW radar is that it can only measure velocity via an object's Doppler shift, but it cannot measure distance. The alternative would be to use a waveform frequency modulated by an external signal. If the transmitter's output is switched on and off periodically between modulated "chirps," the radar is said to operate in pulsed mode. If the modulated emission is continuous, the radar uses FMCW. We elected to build an FMCW radar because it offers accurate range measurements without the complicated switching circuitry and waveform design of a pulsed radar. When designing the processing unit, we required a microcontroller capable of both generating and capturing analog signals with high fidelity. We chose the Microchip PIC18F56Q71 because of its low power consumption and high-resolution ADC and DAC. To log data, we used an off-the-shelf SPI-compatible SD card module, along with a barometric altimeter module. In practice, we did not use these components, as we could not communicate with them while generating a DAC signal and sampling the ADC signal. To power the entire system, we chose a high-efficiency boost converter to produce a 10V bus. This 10V was fed to 3V, 3.3V, and 5V LDOs that powered the VCO, microcontroller, and amplifiers, respectively. Using LDOs was necessary to provide a low-noise supply to the sensitive analog circuitry contained in these components.

To verify the functionality of our RF designs, we simulated our boards and antennas in Ansys HFSS electromagnetic solver software and Keysight ADS design software.

2.3 Design Details

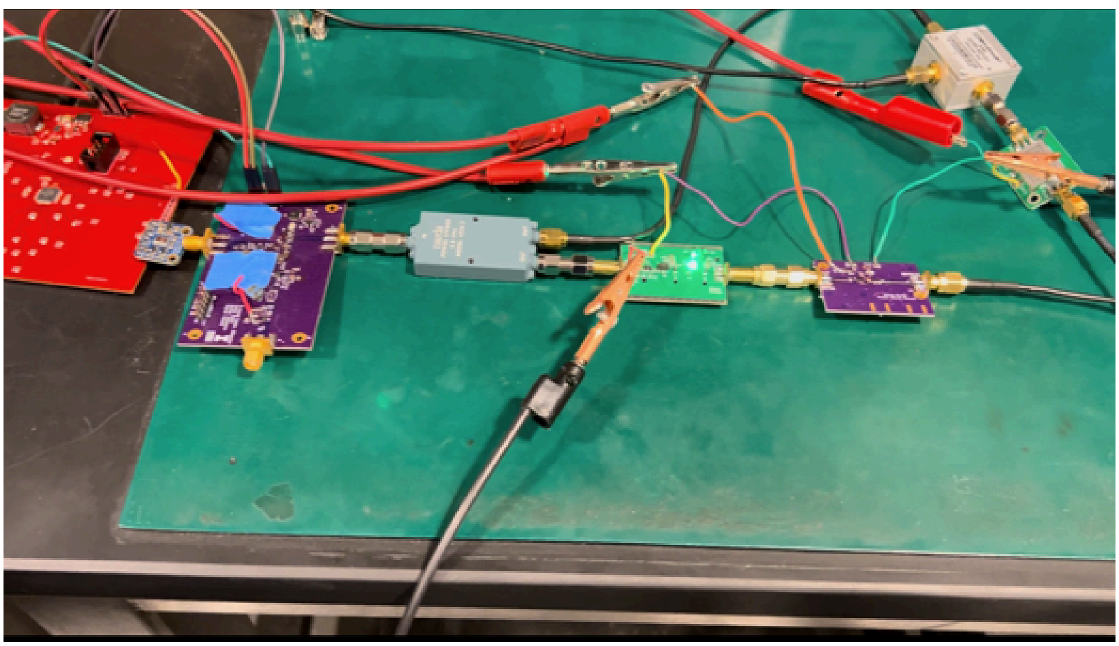

Figure 3: Final System Construction, From Left to Right: Power/Processing Unit, VCO Board, Power Divider, Power Amplifier, LNA, Mixer

2.3.1 Radar Unit

The radar unit consists of the transmitter subsystem and the receiver subsystem. A simple description of the radar unit is as follows:

The radar board receives a control signal from the DAC on the processing unit. This control signal connects to the VCO and generates a FM sweep, which is used by the transmitter to send FMCW pulses. The receiver also uses this FM sweep as the LO for demodulating the FM pulses. The LO is fed into a mixer which creates a low-frequency IF signal. The IF signal is filtered, amplified, and connected back to the processing unit. Finally, the IF signal is sampled by the processing unit to obtain range and velocity information.

The transmitter subsystem is responsible for generating and transmitting FMCW waveforms used in the radar. A VCO, driven by a triangle wave from the microcontroller, creates an FM signal over a specified bandwidth from 100 MHZ - 250 MHz. This waveform is split off by a directional coupler to be used as the LO (local oscillator) in the receiver subsystem. A lowpass filter is used to attenuate the VCO second harmonic before it reaches the coupler. Finally, a PA amplifies the signal to be transmitted by the antenna. We chose to use the HMC385 VCO [4] which operates between 2.1 and 2.7 GHz, and is somewhat linear between 2.2 and 2.5 GHz – our desired operating range. For the PA, we chose to use the GRF4002W [1] which has 15 dB of gain and a 1 dB compression point of 23.5 dBm at 2.5 GHz with a 5V supply. Conveniently, the GRF4002W has a noise figure of 0.85 dB under these conditions, making it suitable for use in the receiver as well. The receiver subsystem is responsible for receiving and demodulating the reflected FMCW signal from the target. It consists of a LNA, a mixer, and an active IF filter. The mixer LO port is driven by the transmitted signal to produce small sum and difference frequencies used in range calculation. The IF filter cleans the demodulated signal so it can be sampled by the microcontroller ADC without aliasing. The IF filter itself is located on a small circuit card that mates with the radar board. In our final design, we did not use the IF filter for reasons mentioned in sections 2.1.1 and 2.2. Originally, we used a directional coupler to drive the mixer's LO input. However, in our final design, we opted to use a 2-way power divider instead for lower loss. Likewise, we used an off-the-shelf mixer and LNA in our final design. Schematics and layouts of our second and third RF designs are shown in Appendix D.

Although we originally planned to build Yagi-Uda antennas, we instead built "cantennas" because they were easier to manufacture. These simple aperture antennas provide approximately 9 dB of gain at 2.5 GHz, and are well matched to 50 Ω. This design, which we optimized in HFSS, is based on a detailed treatment of circular aperture antennas found in [2]. The results of this design are shown in Appendix A.

2.3.2 Power Unit

The power unit subsystem is responsible for distributing necessary power to the radar and processing unit. A 3.7V lithium ion battery was initially proposed to supply power to the entire system. However, after initial design stages it was decided that we did not possess a safe way to charge said battery. We instead opted to use external power supplies. A buck-boost converter will take the 3.7V bench power supply as an input and step up to 10V. This 10V output is then fed into two other LDOs, one to convert to 3V and another to convert to 3.3V. The 10V output is used to power an op-amp on the radar unit, and was also originally used to power a 5V LDO on the radar unit as well. Although it remained populated on the radar board, we did not use the 5V LDO. The schematic and layout for this part of the board is shown in Appendix D.

2.3.3 Processing Unit

This subsystem is responsible for receiving a signal from a low pass filter and going to a microcontroller. The microcontroller contains an analog-to-digital converter within the chip. After the signal becomes digital, it is used to calculate the height from the ground using the time shift equation from eq. 1. This information is transferred to an SD card using the SPI communication protocol. Also included is a barometric altitude sensor which gives the true height of the radar. This information is transferred to the microcontroller using the I2C communication protocol. In our design, we were unable to realize a working PIC microcontroller operating on its own without the use of a development board. We also did not use our barometric sensor and micro SD card. Although we did not use our actual PIC microcontroller, we still designed one and placed it on our development board along with connections to our radar unit, barometric sensor and SD Card. The schematic and layout for this part of the board is shown in Appendix D.

2.4 Costs, Schedule, and Labor

Labor:
A typical graduate student at the ECE department makes approximately $2,800 per month. Breaking this figure down even further this comes out to $700 per week. Since ECE graduates work part-time (20 hours per week), they make approximately $35 per hour. If we benchmark this number and say that each individual in our senior design group is getting paid $35 an hour, we can come up with a number for total labor cost.

Throughout the course of this project each team member averaged ~12.5 hours per week working on this project. Therefore, the total labor cost per person = 2.5 x $35/hour x 12.5 hours/week x 14 weeks. This evaluates to a total cost per person of $15,312.5. Along with $302.43 in parts, some of which we purchased ourselves, the total cost of this project including labor is $46,239.93. The total cost breakdown is shown in Appendix C.

Schedule:

Task	Member(s)	Description	Timeline
RF Board	Elliot	Design schematic and complete RF board layout	Complete by week of February 26th
IF Board	Elliot	Design schematic and complete IF board layout	Complete by week of February 26th
Power and Processing Board	Bobby Rayan	Design schematic and complete Power and Processing board layout	Complete by week of February 26th
Order PCBs	Bobby	Order PCBs from PCBway	Complete by March 5th
Order Individual Components	Elliot	Order all discrete components	Complete by March 5th
Simulations	Elliot Bobby	Conduct simulations in HFSS and ADS to assess expected performance	Complete during wait time of PCB delivery
MCU Analog Software Creation	Rayan	Start writing code to control ADC/DAC of MCU	Complete during wait time of PCB delivery
Soldering Components	Everyone	Solder all discrete parts onto each PCB	Complete by week of March 25th
Assemble Design	Everyone	Assemble all three PCBs and system chassis into one system	Complete by week of March 25th
Test Design	Everyone	Conduct tests on design and compare against simulations	Complete by week of March 25th

MCU SD Card/Barometer code	Rayan	Write code to interface with SD card and barometric altimeter	Complete by April 2nd
Modify and Reorder Design (if necessary)	Elliot Bobby	Modify and reorder design to improve performance	Complete by April 2nd
Test Design Again	Everyone	Conduct tests on design and compare against simulations	Complete by week of April 8th
Demo	Everyone	Demo final board	Complete by April 24th
Presentation	Everyone	Conduct final presentation	Complete by April 30th
Final Paper	Everyone	Turn in final paper	Complete by May 1st

Table 1: Semester Project Schedule

3. Verification

3.1 Radar Unit

In order to ensure RF performance, the following requirements were imposed on the radar unit:

1. The radar unit must consume fewer than 2W when in operating mode.
2. The VCO second harmonic must not exceed -20 dBc.
3. The PA and LNA must be stable across the whole 2.25 GHz - 2.5 GHz operating band.

Requirement 1 was verified by powering the entire system from a bench supply and observing the measured power on the screen. We connected the VCO, transmitter, and receiver to 3V and 5V, respectively. In this test, we drove the PA directly with the VCO to most accurately represent its behavior in operating mode. We looped back the PA output through an attenuator to the LNA input. Then, we added up the power dissipation from the 5V RF supplies plus the 3V VCO supply, which was found to be 1.98 W.

Requirement 2 was verified by observing the VCO output spectrum on a signal analyzer. The second harmonic amplitude varies with VCO output frequency, so we swept the VCO tuning pin with a ramp signal between 0 and 10V. We set the signal analyzer trace mode to max hold and observed the resulting spectra. The VCO second harmonic was observed to be on the order of 40 dB down from the fundamental frequency across the entire VCO sweep, thus exceeding the -20 dBc spec.

Requirement 3 was verified by measuring the PA and LNA frequency responses using a network analyzer. We calibrated the network analyzer for a 2-port measurement with a sweep range of 100 kHz - 3.8 GHz and an IF bandwidth of 10 kHz. Ensuring that the network analyzer's output was turned off, we connected the PA to the network analyzer and powered on the PA using 5V from a bench supply. We then enabled the network analyzer output and plotted the μ stability factor. We found μ to be greater than 1 for 2.25 - 2.5 GHz, thus satisfying the stability criterion outlined in [6]. This test was repeated in the exact same manner for the LNA, which also was stable for 2.25 - 2.5 GHz.

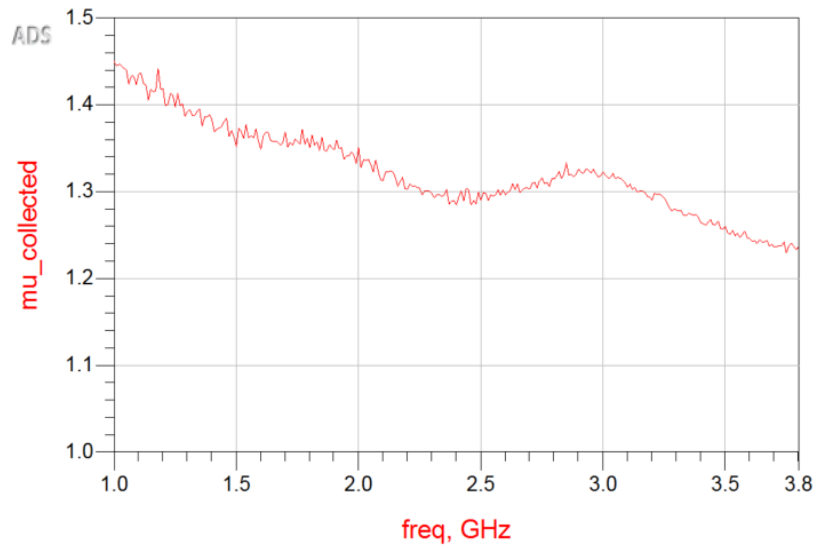

Figure 4: PA/LNA Stability Factor, μ, Captured From Network Analyzer and Plotted in ADS

3.2 Power Unit

For the power unit, there were 5 subsystem level requirements which we aimed to achieve:

1. Reverse Polarity Protection
2. Fuse that will operate when more than 2.5A of current flows through it
3. Undervoltage protection
4. Less than 0.2V ripple for 10V supply
5. Less than 0.1V ripple for 3V, 3.3V and 5V for the voltage regulators

In order to test for reverse polarity we connected 3.7V across the smart diode in reverse to check that it acted as an open circuit. This test was successful as the diode did act as an open circuit. The next verification which we performed was that of the fuse. This test was straightforward as all we needed to do was run 2.5A of current and see if the fuse opens. We did not follow through on testing under voltage protection because we did not use the Li-Ion battery. Finally, in order to test the ripple on the voltage regulators we used an oscilloscope and set markers to look at the ripple voltages. We were able to pass the test with the ripple voltage. Overall, all tests passed for the power unit except that of the undervoltage protection because we did not end up using the Li-Ion battery.

3.3 Processing Unit

The requirement imposed on the processing unit was that it must have an error rate of less than 10% to be considered successful. In order to verify this subsystem requirement, we broke this down into a sequence of steps.

The first step was to check to see if we were successfully able to send data using SPI communication protocol. In order to do this, we created a test vector in our code in the main.c function in order to check that the sequence of strings being transmitted was the same as that in our test vector. Finally, we sent a waveform through the PIC microcontroller which was attached to a development board and hooked the output into Analog Devices SCOPY software via a USB oscilloscope. We then downloaded the code onto our microcontroller and hit run on SCOPY. This test was successful as we were able to see the same data in the test vector as in SCOPY.

Figure 5: Test Vector SCOPY Output

The second step was to use SCOPY in order to see if we could have the ADC code and SPI working simultaneously. When verifying this, our setup was exactly the same as when we tested SPI by itself. The results for this test were interesting as we were able to see packets being received by the logic analyzer. However, the samples in the packets were incorrect as a result of aliasing. We determined that the ADC was bottlenecked by SPI transactions and would be unable to sample fast enough to recover an input signal above ~1kHz.

After realizing that our ADC was not able to sample at a fast enough rate using the PIC microcontroller we tried the Arduino Uno to see if we could read digital values at the desired rate. Unfortunately we observed the same result and were unable to implement this feature.

4. Conclusions

4.1 Accomplishments

Throughout the course of this project, we as a group have learned a tremendous amount about the engineering design process as well as RF/Microwave design considerations. The continuous reworking and fabrication of new iterations of the RF board showed us how sensitive higher frequency circuitry can truly be compared to what we have worked with in prior lab courses. The power and processing boards proved to be a much easier endeavor to layout and fabricate than the RF board, but the coding and flashing of the PIC microcontroller was the true bottle neck of the project. We discuss in the next section how we would remedy this failure if given the opportunity to work on this project again. Even though we were unable to achieve 100% functionality we were still quite happy to be able to see our system respond to different range values through the use of an oscilloscope.

4.2 Future Work

In order to make this radar unit fully functional, several changes need to be made to the radar unit and the processing unit. Starting with the radar unit, it would be beneficial to use the VCO as part of a phase locked loop (PLL) [5], to linearize its tuning behavior. This gives a much cleaner frequency sweep, removing harmonic content from the IF signal. As a result, the strain on the anti-aliasing filter would be reduced and the ADC would have an easier time sampling the IF signal. A PLL-based frequency sweep would also make calculating range and velocity much easier, since we would not have to guess what the VCO output frequency is for a given voltage as the voltage-frequency relationship is nonlinear. In retrospect, we would change our microcontroller to an ESP32, STM32, or similarly well-supported hardware platform. These microcontrollers are widely used and well-documented, so we would save time developing our firmware. Next, we would add a battery management system to the power unit, ensuring that we can safely charge the Lithium battery. While the battery that we selected does have a rudimentary discharge, overvoltage and undervoltage protection system, we do not presently have a way to charge it properly. Finally, the most critical change to make on the next revision of this project would be to break the entire RF system into separate modules for each component. We did this for the amplifiers in our final board revision, but it would have been incredibly helpful if we had done this for the VCO and mixer components as well. This would have saved us many hours of debugging, since we had no way to isolate RF problems that affected multiple components.

4.3 Ethical Considerations

When developing an S-band radar altimeter for drone height detection, several ethical and safety considerations must be addressed. These considerations encompass both the development process and the potential misuse of the technology.

A significant concern relates to measurement accuracy, and the implications of the radar's measurements. Inaccurate height measurements could lead to dangerous decisions based on erroneous data. In extreme cases, inaccurate altitude data could cause injuries and destruction of both the radar and the drone. This is a potential conflict with section 1.2 in ACM's Code of Ethics [9], which mandates engineers to avoid harm wherever possible. If this product were to be sold to consumers, we would need to implement an accurate method of altitude calculation beyond just using an oscilloscope. This would need to be benchmarked against a similar radar or other range detection system.

A related safety issue pertaining to I-1 of [7] is that of RF interference. Our device operates in the S-band, which is widely used by aircraft, RC vehicles, cellular infrastructure, WiFi, and Bluetooth. Additional harmonic content generated by our radar may leak into adjacent GPS or cellular bands, affecting signal quality. For this reason, we placed a filter at the output of our VCO to attenuate spurious content that might leak into other channels. Additionally, we designed our antennas to be as directive as possible so that we can control where they are radiating, to some degree.

Finally, in the development of prototypes or experimental hardware such as our radar, it is critical that our team is open to extensive review of our design. This is directly pursuant to section I-5 of the IEEE Code of Ethics, which mandates that we accept constructive feedback and make informed design choices based on all available data [7]. To abide by this rule, we made sure to consult professors, experts, and TAs regarding the more challenging aspects of our design. Additionally, we thoroughly simulated our design so that we could iterate it in the most informed way possible.

References

[1]“GRF4002-W Data Sheet | Guerrilla RF,” *www.guerrilla-rf.com*, Sep. 12, 2023. https://www.guerrilla-rf.com/products/DataSheet?sku=4002-W&file_name=GRF4002WDS.pdf (accessed May 01, 2024).

[2]W. L. Stutzman and G. A. Thiele, *Antenna theory and design*. Hoboken, Nj: Wiley, 2013.

[3]I. Rosu and F. Rosu, “S-Band 2.4GHz FMCW Radar.” Accessed: May 01, 2024. [Online]. Available:https://www.qsl.net/va3iul/Radar/S-Band_2.4GHz_FMCW_Radar/S-Band_2.4GHz_FMCW_Radar.pdf

[4]“HMC385 Datasheet,” *Analog Devices*, Apr. 22, 2015. https://www.analog.com/media/en/technical-documentation/data-sheets/hmc385.pdf (accessed May 01, 2024).

[5]H. Forstén, “Third version of homemade 6 GHz FMCW radar,” *Henrik's Blog*, Sep. 28, 2017. https://hforsten.com/third-version-of-homemade-6-ghz-fmcw-radar.html (accessed May 01, 2024).

[6]S. Franke, *ECE 453: Wireless Communications Systems*. University of Illinois at Urbana-Champaign, 2019. Accessed: May 01, 2024. [Online]. Available: https://courses.engr.illinois.edu/ece453/fa2022/

[7]IEEE, “IEEE Code of Ethics,” *ieee.org*, Jun. 2020. https://www.ieee.org/about/corporate/governance/p7-8.html (accessed May 01, 2024).

[8]“User Manual,” DJI. Available: https://dl.djicdn.com/downloads/DJI_Mini_2/20210630/DJI_Mini_2_User_Manual-EN.pdf

[9]ACM, “ACM Code of Ethics and Professional Conduct,” Association for Computing Machinery, Jun. 22, 2018. https://www.acm.org/code-of-ethics

Appendix A Antenna Design

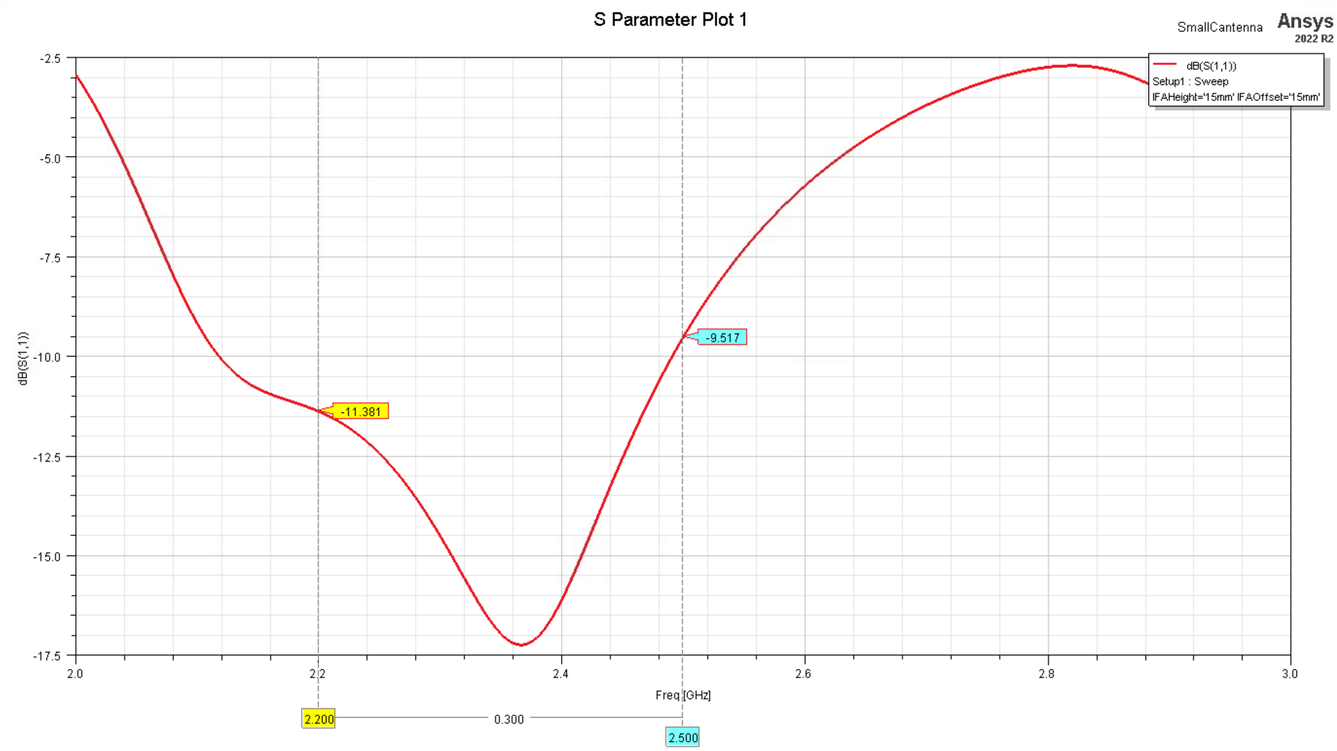

Figure 6: Simulated Antenna Reflection Coefficient From Ansys HFSS

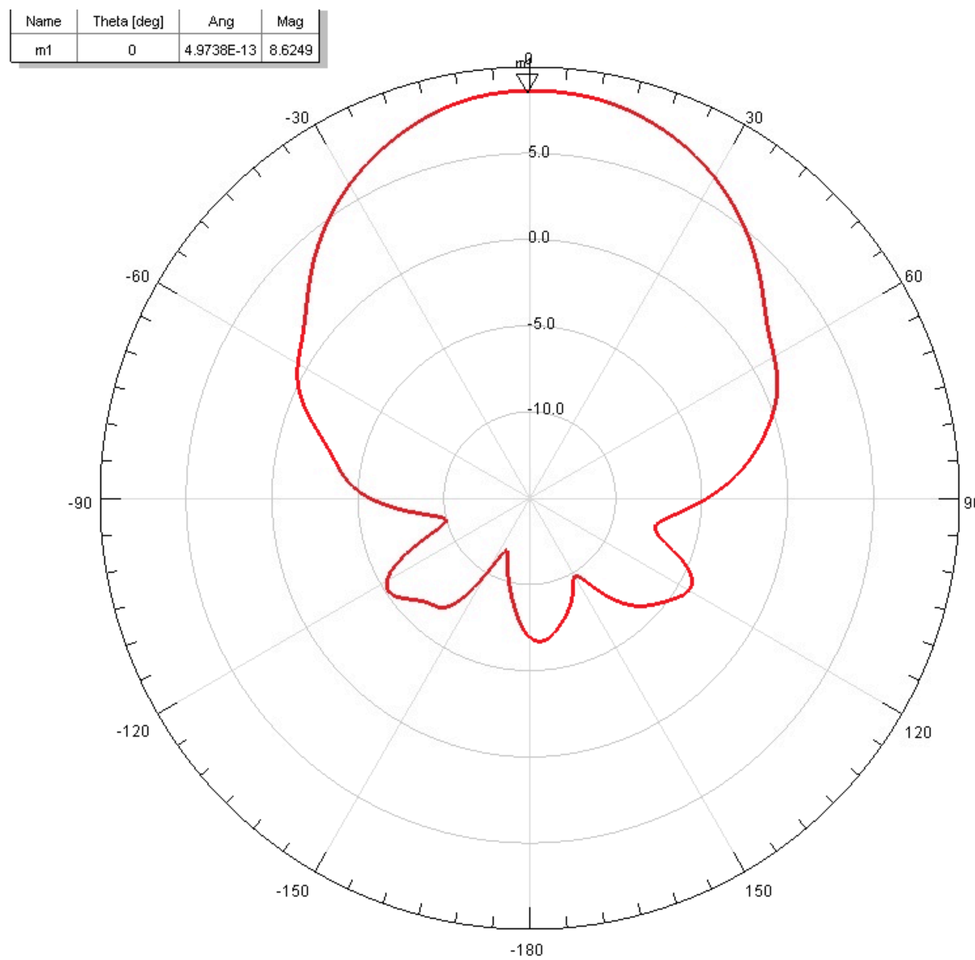

Figure 7: E-Plane Radiation Pattern of Cantenna showing ~8.7 dB of gain

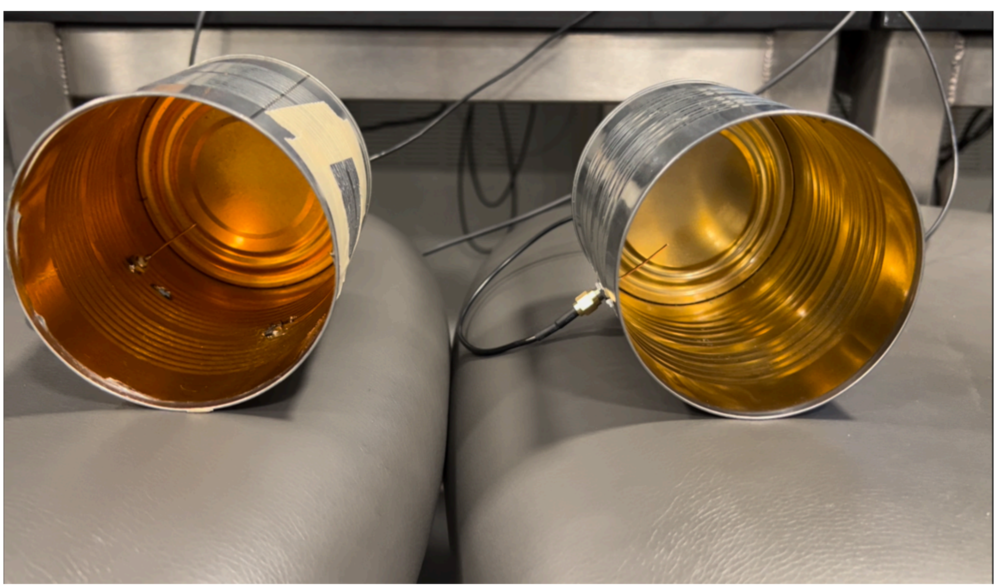

Figure 8: Final Cantenna Design

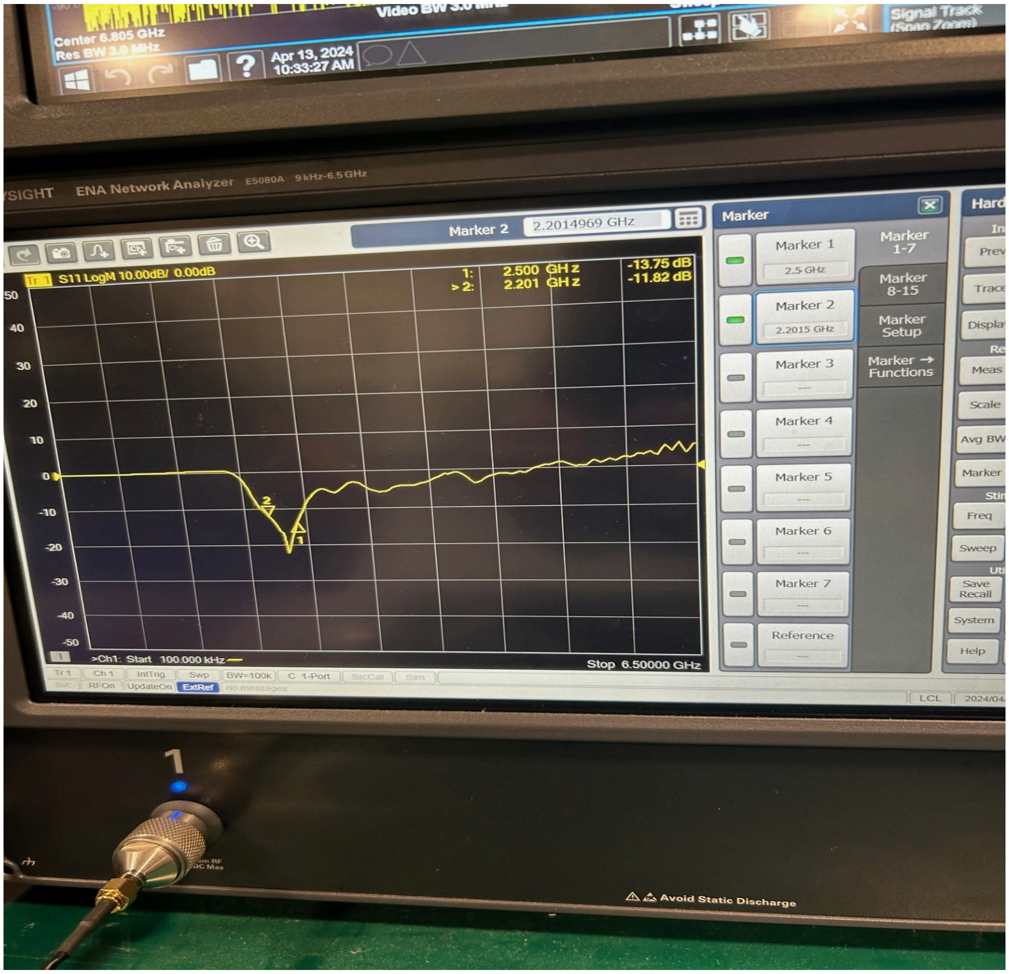

Figure 9: Measured Reflection Coefficient of Cantenna

Appendix B Requirement and Verification Table

Requirement	Verification Method	Verification Result
Radar unit must consume fewer than 2W of power in operating mode	Observe radar unit power draw on bench supply; add up total system power	Pass
VCO second harmonic must not exceed -20 dBc relative to fundamental	Measure VCO second harmonic amplitude relative to fundamental frequency using spectrum analyzer	Pass
PA and LNA must be stable across 2.25-2.5 GHz operating band	Measure amplifier μ stability factor using vector network analyzer and ensure $\mu > 1$	Pass

Table 2: Radar Unit Requirement and Verification Table

Requirement	Verification Method	Verification Result
Power unit must include reverse polarity protection capable of stopping reverse current flow at 3.7V	Connect 3.7V power supply to terminals in reverse; observe current draw on power supply	Pass
Power unit must include a fuse which opens if over 2.5A are drawn	Set power supply current limit to > 2.5A at 3.7V, connect fuse between positive and negative terminals, observe if fuse opens	Pass
Power unit must contain undervoltage protection which stops current flow for supply voltage under 3V	Apply fewer than 3V to power unit terminals and observe current draw	Fail
The DC-DC converter must be able to supply 10V with fewer than 0.2Vpp ripple at 2A maximum current	Observe DC-DC converter output on oscilloscope, observe peak to peak voltage ripple at 2A load	Pass
The 3.3V LDO, the 5V LDO, and the 3V LDO must also be able to supply their respective voltages with < 0.1 Vpp ripple	Load LDOs with maximum rated currents, observe peak to peak voltage ripple on oscilloscope	Pass

Table 3: Power Unit Requirement and Verification Table

Requirement	Verification Method	Verification Result
Processing unit must have an error rate of less than 10%; errors occur when calculated radar altitude is not within 5% of barometric altimeter reading	Save data from both radar altimeter measurement and barometric altimeter measurement onto SD card; determine % difference between altimeter and barometric sensor	Fail

Table 4: Processing Unit Requirement and Verification Table

Appendix C Component Costs Table

Part Name	Vendor	Quantity	Description	Price	Total Price
HMC213B*	Analog Devices	1	Mixer 1.5-4.5 GHz	$0.00	$0.00
TCCH-80+	Mini Circuits	1	RF Choke	$4.91	$4.91
BLM15PX121BH1D	Murata	6	100☐ ferrite	$0.31	$1.86
LFCN-2750+	Mini Circuits	1	Bandpass filter DC-2750 MHz	$2.97	$2.97
HMC385LP4*	Analog Devices	1	VCO 2.25-2.5 GHz	$0.00	$0.00
AZ1084CD-5.0TRG1	Diodes, Inc.	1	LDO 5V 5A	$0.56	$0.56
GRF4002	Guerilla RF	4	RF Amp 0.1-3.8GHz	$2.56	$10.24
DCW-11-722+	Mini Circuits	2	Directional Coupler	$4.17	$8.34
TRF37A73IDSGR	Texas Instruments	1	RF Amp 0.001-6GHz	$1.44	$1.44
PSA-5453+	Mini Circuits	1	RF Amp	$1.96	$1.96
TS461CLT	STM	1	Op-Amp	$1.07	$1.07
73251-1153	Molex	3	SMA Connector	$3.94	$11.82
PH1-05-UA	Adamtech	10	CONN HEADER VERT 5POS 2.54MM	$0.10	$0.99
LT6202CS8#PBF	Analog Devices	2	Op-Amp	$5.25	$10.50
AD8031ARTZ-REEL7	Analog Devices	1	Op-Amp	$3.77	$3.77
U.FL-R-SMT-1(80)	Hirose Electric	1	U.FL Connector	$0.22	$0.22
TPS61230ARNSR	Texas Instruments	1	Buck-Boost Converter	$1.96	$1.96
AZ1117CH2-3.3TRG1	Diodes Incorporated	1	LDO	$0.35	$0.35
AP7375-50SA-7	Diodes Incorporated	1	LDO	$0.41	$0.41
MIKROE-698	MikroElektronika	1	3.7V Li-Ion Battery 1Ah	$8.90	$8.90

DEV-13743	Sparkfun	1	SD Card Shield	$5.95	$5.95
MPL115A2	Adafruit	1	Barometric Altimeter Shield	$9.95	$9.95
PIC24FJ128GC010-I_PT	Microchip Technologies	1	MCU	$0.00	$0.00
GRT155R60J106ME13J	Murata	10	0402 ceramic cap 10u	$0.22	$2.23
GRM155D81A475ME15J	Murata	10	0402 ceramic cap 4.7u	$0.09	$0.90
GRM155C71C105ME11D	Murata	10	0402 ceramic cap 1u	$0.05	$0.50
GRM152R61A104KE19D	Murata	20	0402 ceramic cap 0.1u	$0.11	$2.18
GRM1555CYA103GE01D	Murata	10	0402 ceramic cap 0.01u	$0.07	$0.68
GRM155R71C153JA01D	Murata	10	0402 ceramic cap 0.015u	$0.03	$0.34
GMD155R71H102KA01D	Murata	10	0402 ceramic cap 1n	$0.58	$5.80
GRM155R61A222KA01D	Murata	10	0402 ceramic cap 2.2n	$0.02	$0.16
GRM155R72A152KA01D	Murata	10	0402 ceramic cap 1.5n	$0.04	$0.37
GRM1555C2A101GA01D	Murata	10	0402 ceramic cap 0.1n	$0.04	$0.39
GRT1555C1E100JA02D	Murata	10	0402 ceramic cap 0.01n	$0.02	$0.22
GJM1555C1H180FB01D	Murata	10	0402 ceramic cap 18p	$0.06	$0.61
GRM1555C1ER50WA01D	Murata	10	0402 ceramic cap 0.5p	$0.05	$0.51
CRT0402-BY-1002GLF	Bourns	10	0402 thin film res 10K	$0.17	$1.69
CR0402-FX-1501GLF	Bourns	10	0402 thin film res 1.5K	$0.01	$0.07
CR0402-JW-681GLF	Bourns	10	0402 thin film res 680	$0.00	$0.01
RP0402BRD074K99L	Yageo	10	0402 thin film res 4.99k	$0.31	$3.07

CR0402-JW-331GLF	Bourns	10	0402 thin film res 330	$0.01	$0.05
RP0402BRD073K3L	Yageo	10	0402 thin film res 3.3k	$0.31	$3.07
RC0402FR-072K2L	Yageo	10	0402 thin film res 2.2k	$0.01	$0.09
RT0603BRE0750RL	Yageo	10	0603 thin film res 50	$0.15	$1.52
RR0510P-101-D	Susumu	10	0402 thin film res 100	$0.03	$0.33
ERJ-2GE0R00X	Panasonic	25	0402 jumper 0 ohm res	$0.02	$0.46
0402HPH-R18XGRW	Coilcraft	2	0402 RF 100n inductor	$2.55	$5.10
0402HPH-R18XGLW	Coilcraft	1	0402 RF 180n inductor	$2.08	$2.08
TPS61288LRQQR	TI	1	10V boost	$1.83	$1.83
PIC18F56Q71-I/PT*	Microchip Technologies	1	Other MCU	$0.00	$0.00
PCBWay Order 1			Est. $40		$40.00
OSHPark Order 2			Est $60		$60.00
OSHPark Order 3			Est $50		$50.00
PIC Nano Board	Microchip Technologies	1	Dev board	$30.00	$30.00
				Total Parts Cost	$302.43
Labor	2.5 x $35/hour x 12.5 hours/week x 14 weeks x 3 group members			**Total Labor Cost**	$45,937.50
				Total Project Cost	$46,239.93

Table 5: Labor and Parts Cost

Appendix D Schematics and Layouts

Schematic and layout PDF begins on the next page.

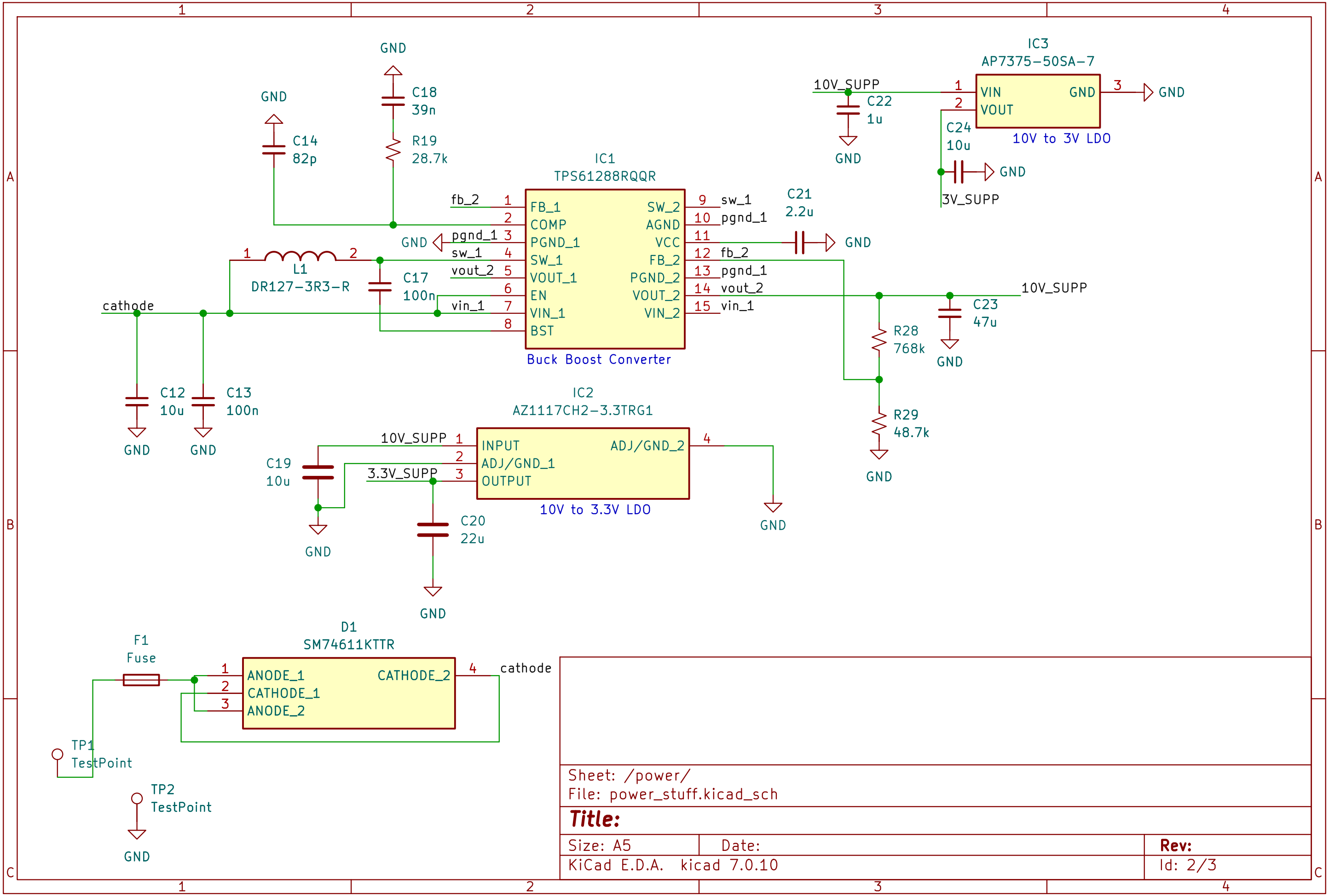

Figure 10: Power Unit Schematic

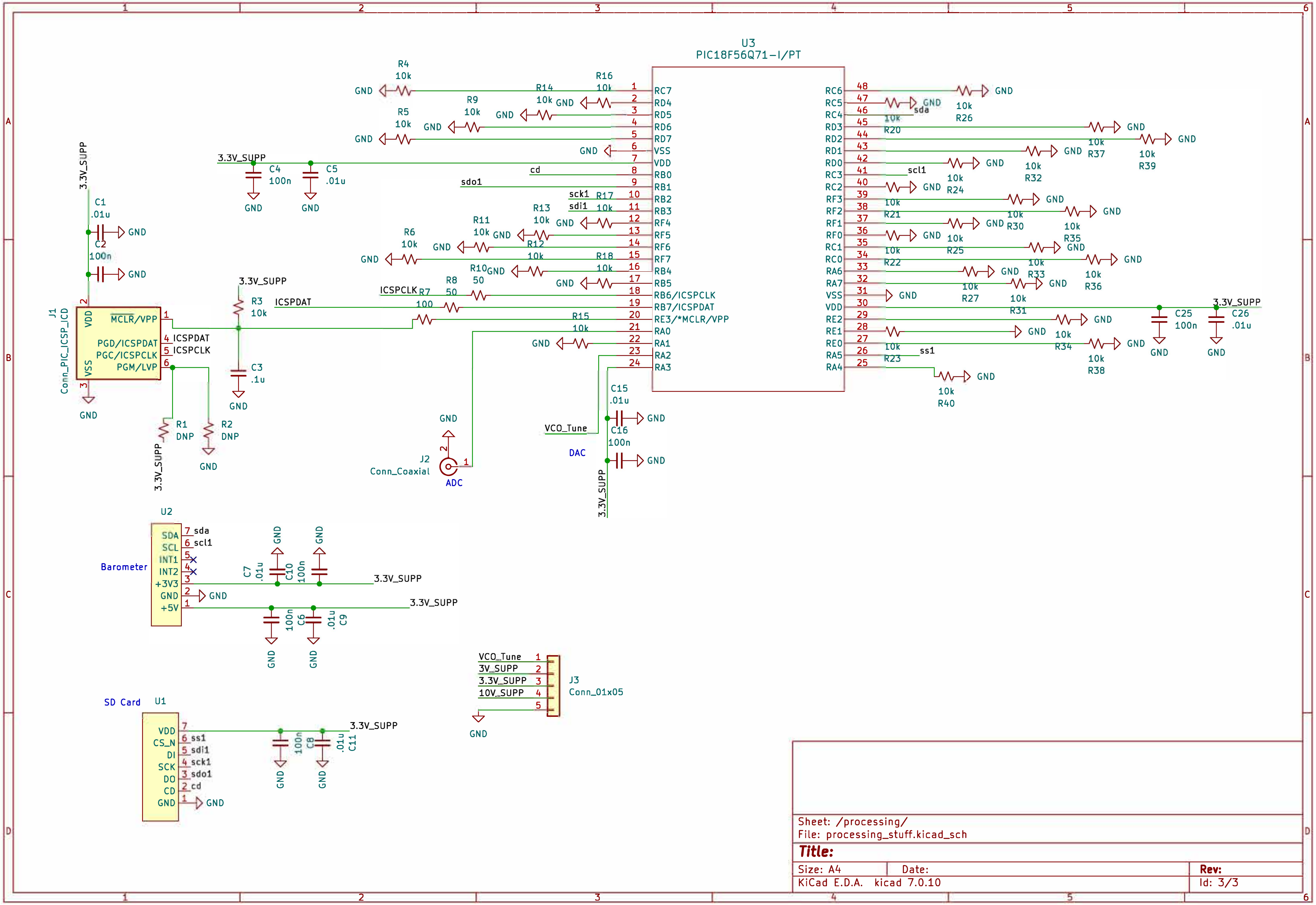

Figure 11: Processing Unit Schematic

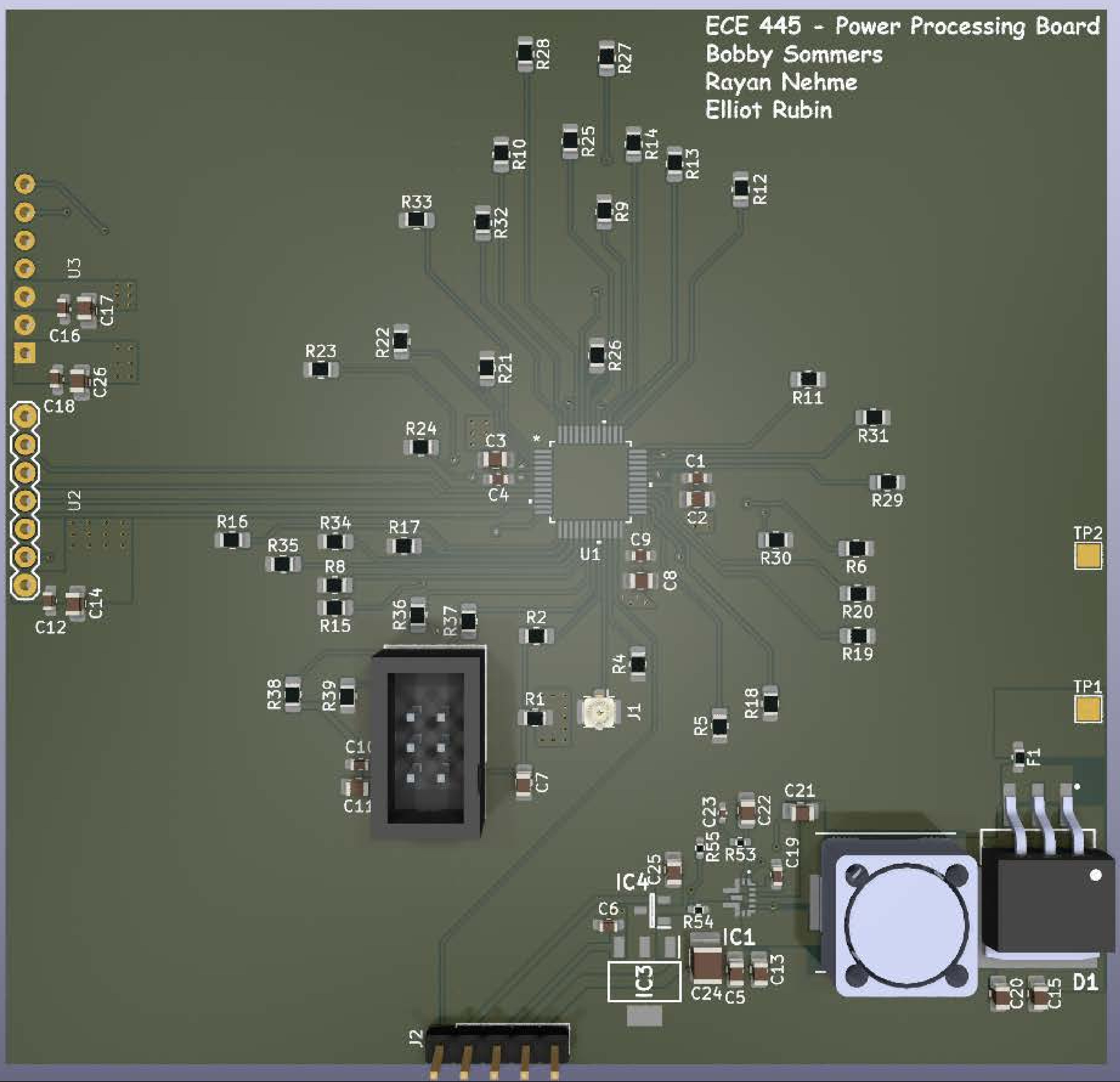

Figure 12: Power/Processing Unit Layout

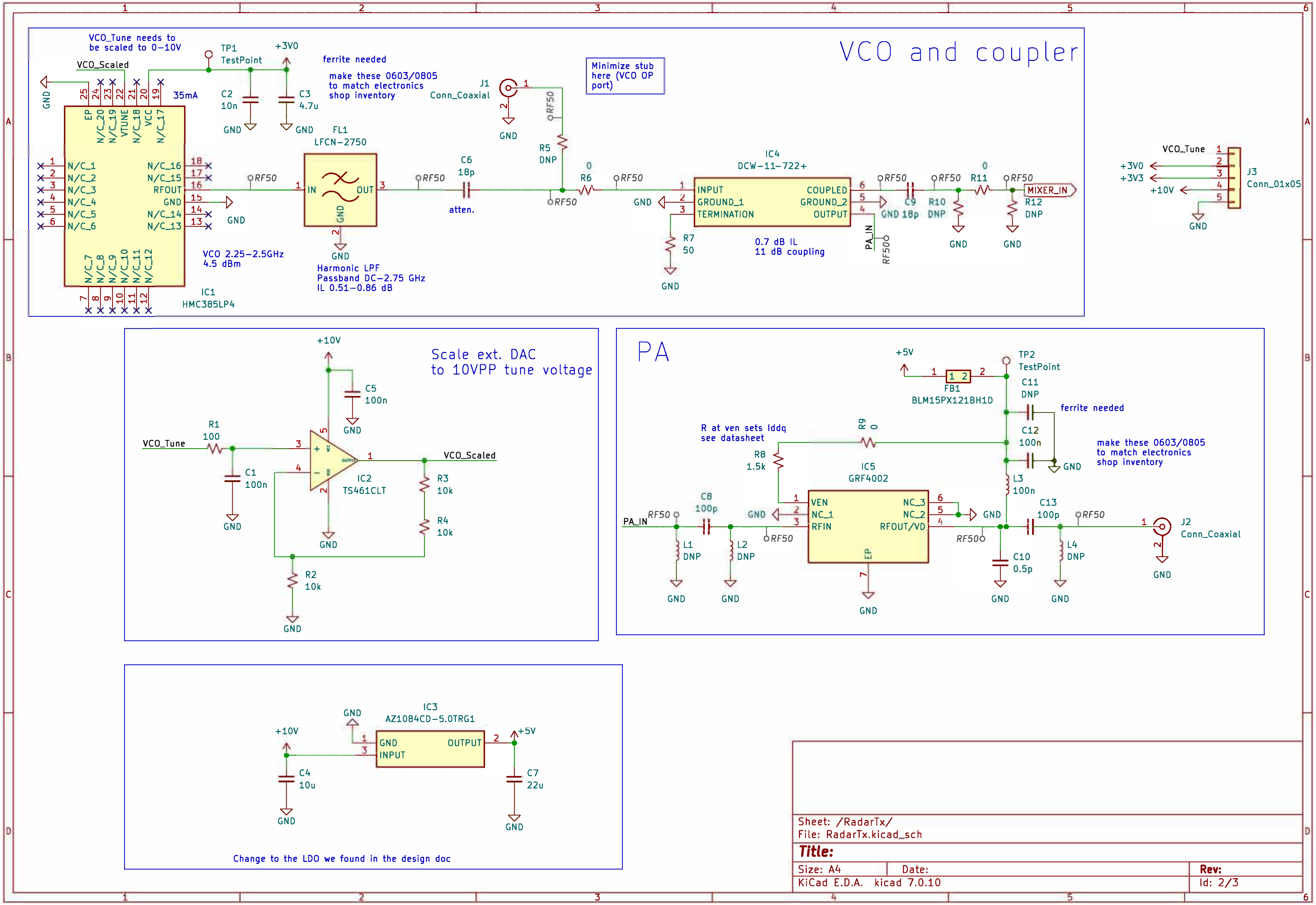

Figure 13: Radar Unit Version 2 Transmitter Schematic - Only the VCO Was Used

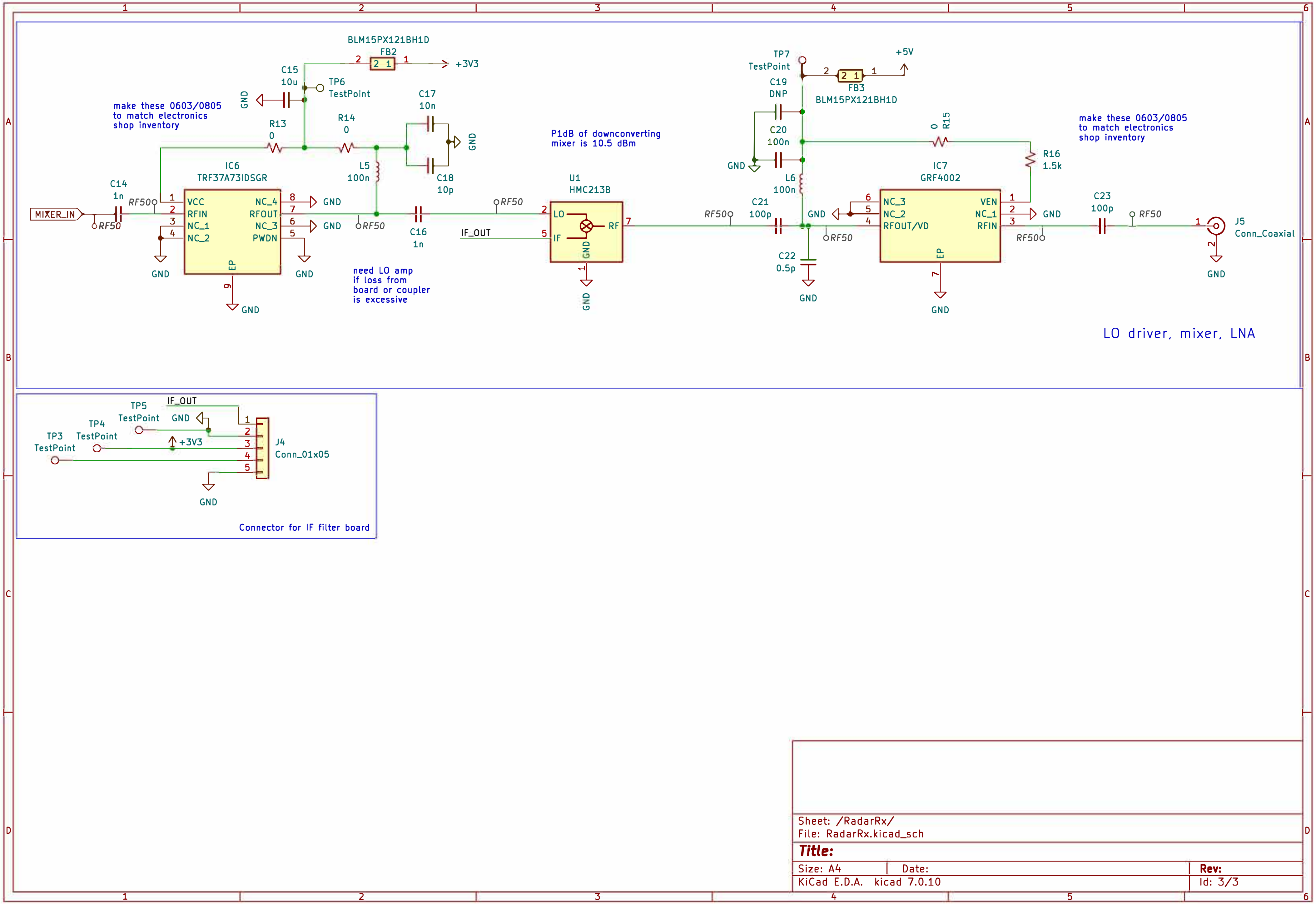

Figure 14: Radar Unit Version 2 Receiver Schematic - Unused in Final Design

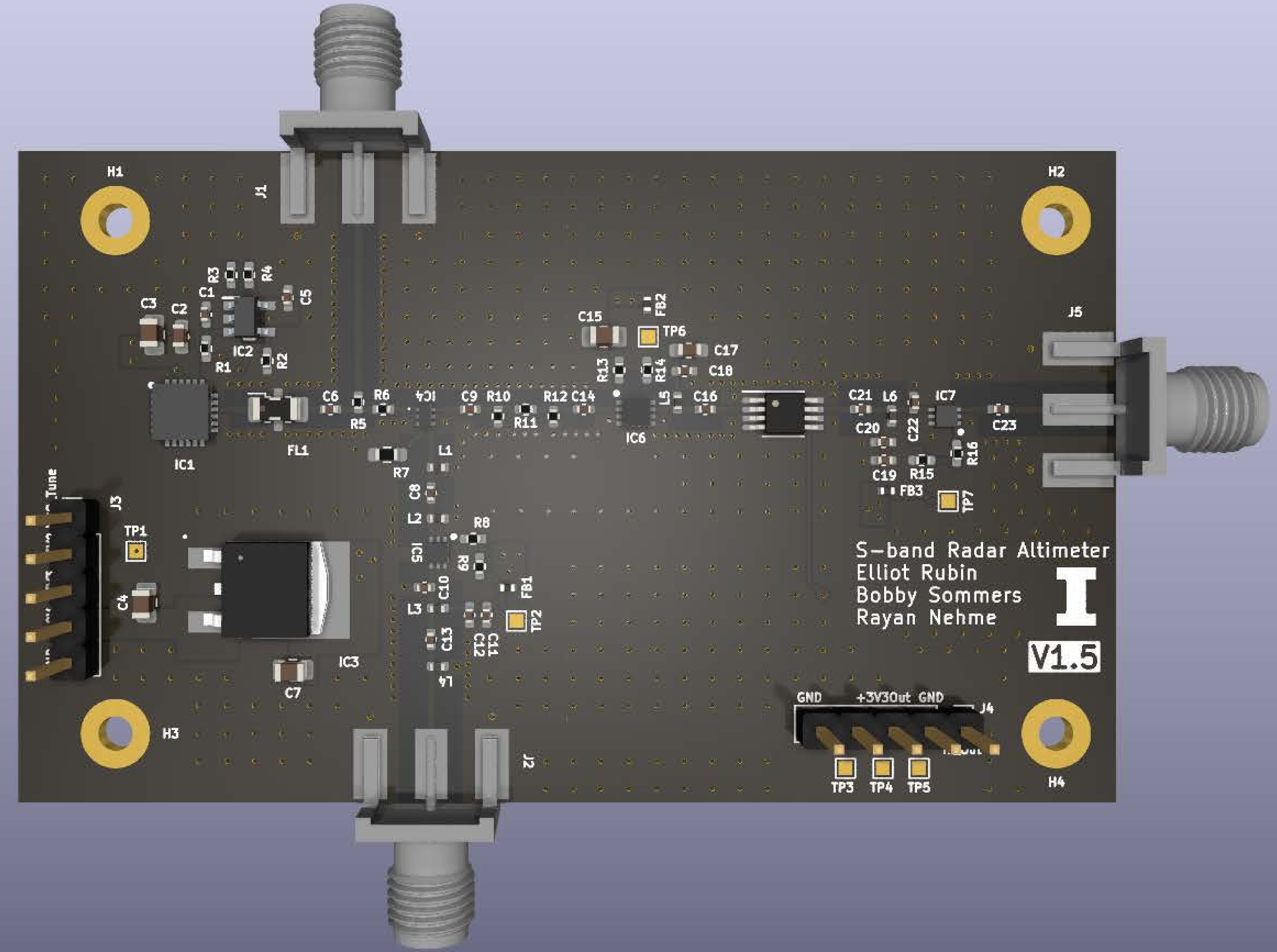

Figure 15: Radar Unit Version 2 Layout

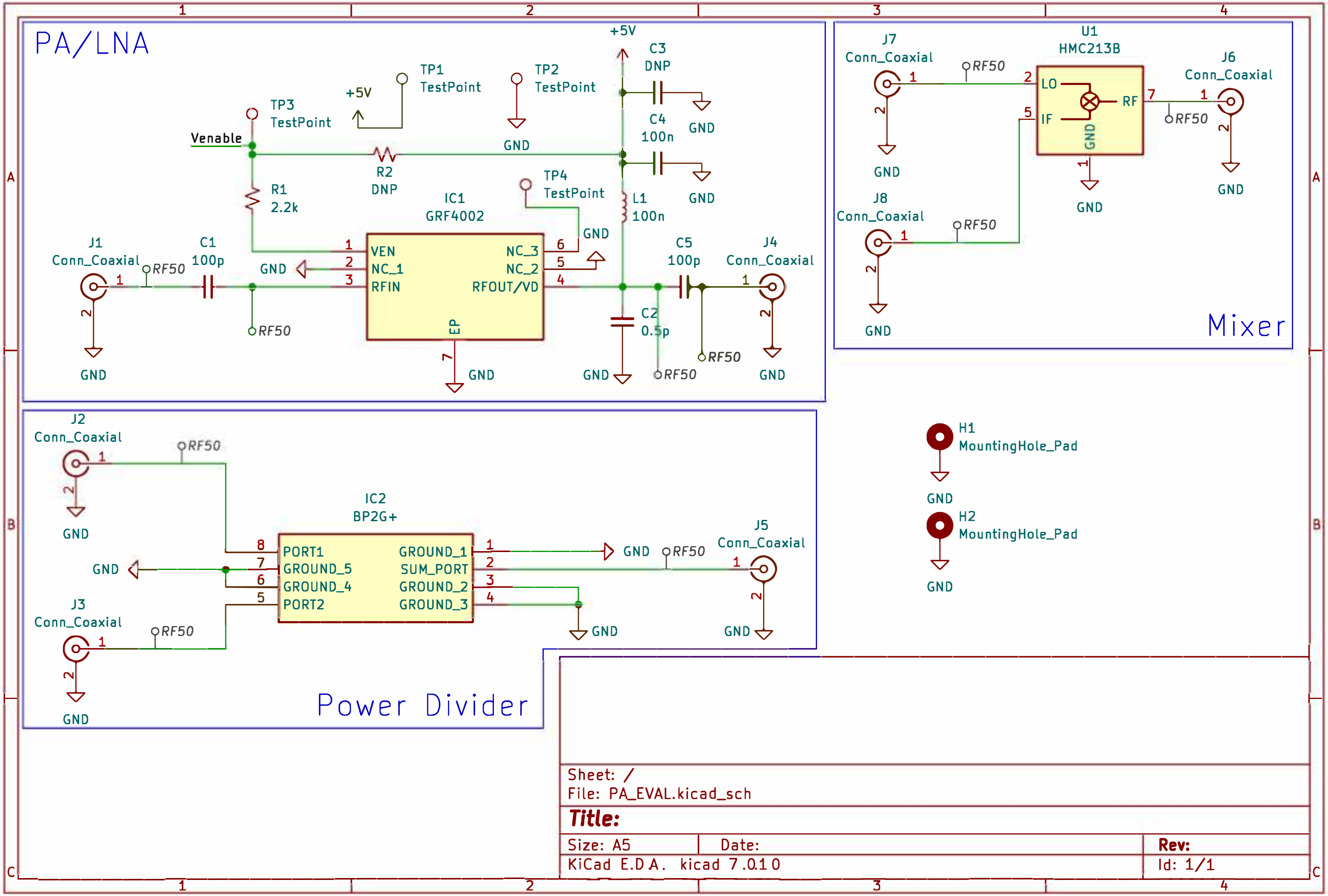

Figure 16: Radar Unit Version 3 Schematic

Figure 17: Radar Unit Version 3 Layout (front)

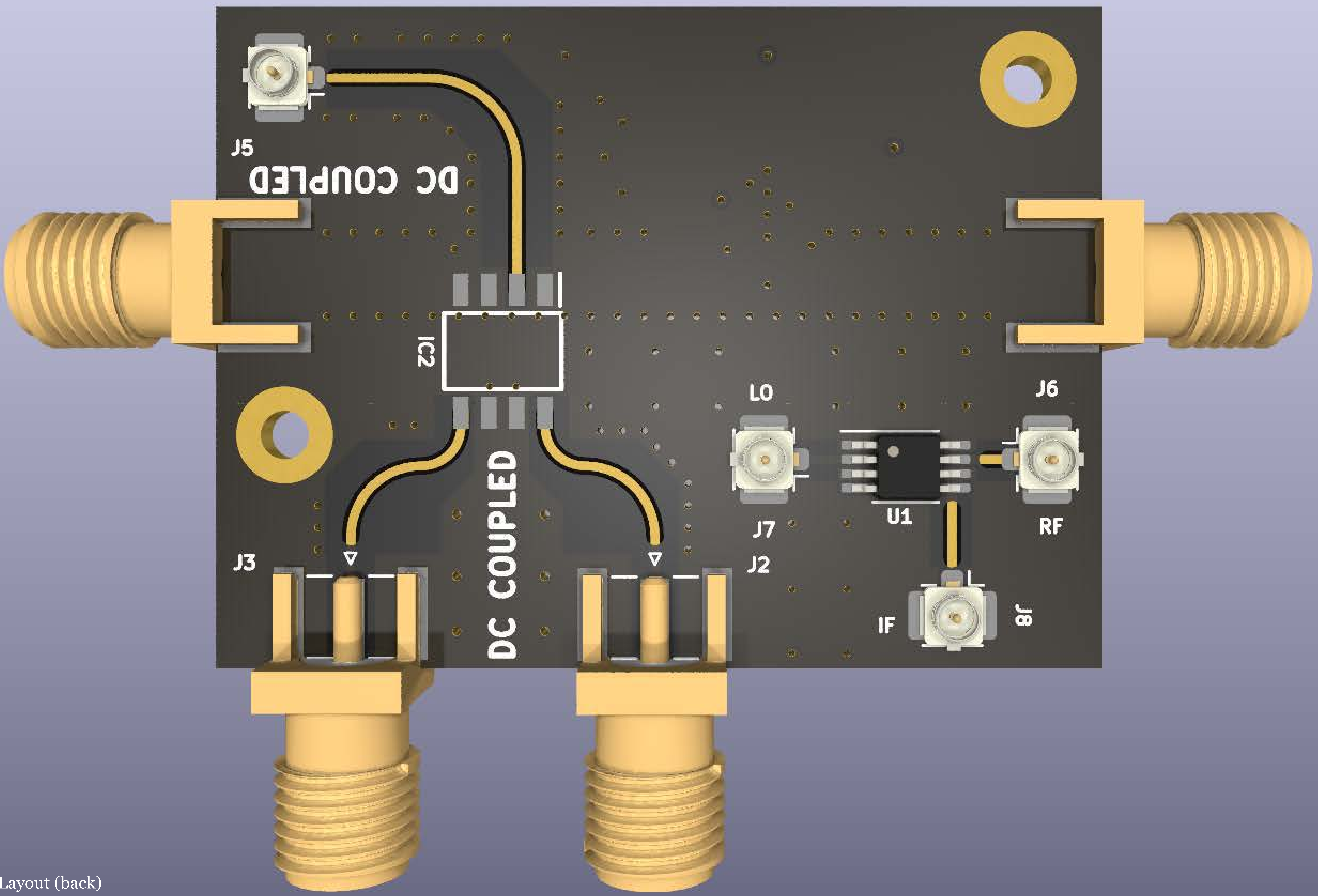

Figure 18: Radar Unit Version 3 Layout (back)